  Bull. Chem. Soc. Jpn., 61, 3159—3167 (1988)

Study of Polarographic Anodic Wave in the Presence of Chloride Ions by a New Numerical Method

Kenji KIKUCHI and Teisuke MURAYAMA*
Shiga Prefectural Junior College, Hikone, Shiga 522
Department of Applied Chemistry, Faculty of Engineering, Shizuoka University, Johoku, Hamamatu 432
(Received January 7, 1988)

A new numerical method is applied to the simultaneous diffusion equations describing the anodic process of mercury in solutions in the presence of chloride ions. The terms corresponding to precipitation and dissolution of mercury(I) chloride are included in the differential equations. It is found that the differential equation for precipitate particles should be rewritten using the backward space difference method for successful computation.

Kolthoff and Miller studied the anodic wave of mercury in the presence of chloride ions.[1] They observed that the diffusion current corrected for residual current is proportional to the concentration of chloride ions. They assumed that the concentration of chloride ions at the surface of mercury electrode is determined by the solubility product and by the concentration of mercury(I) ions at the electrode surface which is controlled by the electrode potential. Based on this assumption they derived an equation of the current-potential curve accompanying with formation of slightly soluble mercury(I) chloride salt as

$$E = E^0 + \frac{RT}{2F} \ln \frac{K_{sp}\gamma_A}{C_{B0}^2} = E' + \frac{RT}{2F} \ln K_{sp} - \frac{RT}{F} \ln (\bar{i}_d - \bar{i}), \quad (1)$$

where E is the potential of dropping mercury electrode, C_{B0} the concentration of chloride ion at the electrode surface, γ_A the activity coefficient of mercury(I) ion, K_{sp} the solubility product of mercury(I) chloride, $\bar{i}$ the average current, $\bar{i}_d$ the average diffusion current, F the Faraday constant, and E^0 the standard electrode potential of Hg_2^{2+}–Hg couple. The plot of $\log(i_d - i)$ vs. E should be a straight line with a reciprocal slope of −59.2 mV/unit at 25 °C. Their plot produced a straight line, however, with a reciprocal slope of −54 mV/unit, which did not agree with Eq. 1.

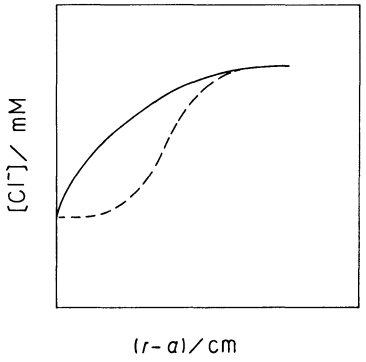

Fig. 1. Distance-concentration curves of chloride ions. A solid line represents a conception considered by Kolthoff and Miller. A dotted line represents a conception proposed by this paper.

After their study, the method and its variations have been generally used for analyzing anodic waves of electrode mercury in the presence of depolarizers which form slightly soluble mercury(I) compounds. The conception proposed by Kolthoff and Miller is that chloride ions are consumed only at the electrode surface and ionic concentration at the electrode surface can be determined by the solubility product and the electrode potential. Figure 1 schematically shows the concentration profile of chloride ions. A solid line was drawn according to their conception. However, chloride ions themselves do not receive any electrochemical change, but are consumed by the chemical reaction with mercury(I) ions produced through the electrochemical reaction. Hence the slope of concentration profile of chloride ions at the surface should be zero as illustrated by the dotted line in Fig. 1. These situations are not reflected in Eq. 1. The equation is a rather crude approximation to the phenomenon, which is waiting more detailed analysis.

This study has two purposes. One is application of a new numerical method,[2] and another is explicit consideration of formation and dissolution of precipitate particles in the process. No direct treatment of dissolution of precipitate particles has been found in literature.

Theory

In the anodic process, mercury is dissolved into solution as mercury(I) ions. When the concentration product of mercury(I) and chloride ions exceeds the solubility product, mercury(I) ions react with chloride ions producing mercury(I) chloride precipitate particles. These reactions are written as follows:

$$2Hg \rightleftharpoons Hg_2^{2+} + 2e^-, \quad (2)$$

and

$$Hg_2^{2+} + 2Cl^- \underset{k_b}{\overset{k_f}{\rightleftharpoons}} Hg_2Cl_2, \quad (3)$$

In Eq. 3, k_f and k_b are rate constants of formation and dissolution, respectively, of the precipitate particles. It is assumed that the effect of formation of mercury(II) ions on the anodic current is negligible in comparison with that of mercury(I) and chloride ions. Further it is assumed that Reaction 3 is rapid and in equilibrium. The solubility product is given by

$$K_{sp} = [Hg_2^{2+}][Cl^-]^2 = k_b[Hg_2Cl_2]/k_f = k_b^*/k_f. \quad (4)$$

Because the solubility of mercury(I) chloride is constant under experimental conditions, the product of the concentration and k_b is replaced by another constant k_b^* in Eq. 4.

In the following, subscripts A, B, and C denote, respectively, mercury(I) ion, chloride ion, and precipitate particle of mercury(I) chloride. Hence their concentrations are expressed as C_A, C_B, and C_C, respectively.

When precipitate particles exist in a volume element considered, or the condition that $C_AC_B^2 \geqq K_{sp}$ is satisfied in the volume element, the simultaneous equations governing concentrations of species appearing in Reactions 2 and 3 are

$$\frac{\partial C_A}{\partial t} = D_A\left(\frac{\partial^2 C_A}{\partial r^2}\right) + \left(\frac{2}{r}D_A - u\right)\frac{\partial C_A}{\partial r} - k_fC_AC_B^2 + k_b^*, \quad (5)$$

$$\frac{\partial C_B}{\partial t} = D_B\left(\frac{\partial^2 C_B}{\partial r^2}\right) + \left(\frac{2}{r}D_B - u\right)\frac{\partial C_B}{\partial r} - 2k_fC_AC_B^2 + 2k_b^*, \quad (6)$$

$$\frac{\partial C_C}{\partial t} = -u\frac{\partial C_C}{\partial r} + k_fC_AC_B - k_b^*, \quad (7)$$

and

$$u = m/(4\pi\rho r^2), \quad (8)$$

where D_h is the diffusion coefficient of species h, r the distance from the center of the electrode mercury drop, m the flow rate of mercury, and ρ the density of mercury. It is assumed that diffusion of the precipitate particles is negligible in comparison with that of ions. The precipitate concentration is expressed in formal concentration of the precipitate substance, which is assumed to be dispersed homogeneously in the volume element. As usually does, it is assumed that the center of mercury drop remains fixed.

When the precipitate does not exist in a volume element, that is $C_AC_B^2 < K_{sp}$, the simultaneous equations describing variation of concentrations are

$$\frac{\partial C_A}{\partial t} = D_A\left(\frac{\partial^2 C_A}{\partial r^2}\right) + \left(\frac{2}{r}D_A - u\right)\frac{\partial C_A}{\partial r}, \quad (9)$$

and

$$\frac{\partial C_B}{\partial t} = D_B\left(\frac{\partial^2 C_B}{\partial r^2}\right) + \left(\frac{2}{r}D_B - u\right)\frac{\partial C_B}{\partial r}. \quad (10)$$

Initial conditions are

$$C_A = 0,\ C_B = C^*_B, \text{ and } C_C = 0\ (t = 0,\ r > a). \quad (11)$$

Boundary conditions are as follows:

$$C_A = C_{A0},\ (\partial C_B/\partial r) = 0\ (t > 0,\ r = a), \quad (12)$$

and

$$C_A = 0,\ C_B = C^*_B,\ C_C = 0\ (t > 0,\ r = \infty). \quad (13)$$

In the above, a is the radius of mercury drop, C^*_B the concentration of chloride ions in bulk solution, and C_{A0} the concentration of mercury(I) ions at the surface of mercury electrode. The potential of mercury electrode dictates the value of C_{A0}. The instantaneous current, i, is given by

$$i = 2FD_AS(\partial C_A/\partial r)_{r=a}, \quad (14)$$

where S is the surface area of mercury drop.

Because the reaction proceeds in the neighborhood of electrode surface, numerical results most desired are those in the proximity of electrode surface. For this purpose, numerical integration of the differential equations is carried out more efficiently using a network, of which mesh is finer in near positions to the electrode surface and becomes coarser with the distance from the surface. Hence we introduce a parameter given by

$$s^P = 1 - 1/\{1 + (Hx)^P\}, \quad (15)$$

where H and P are constants. In the previous report,[2] the value of P is unity.

To facilitate calculation, we introduce the following transformations:[2]

$$y_A = C_A/C_{A0},\ y_B = C_B/C_{A0},$$
$$y_C = C_C/C_{A0},\ x = (r - a)/L,$$
$$d_A = D_A/D_A = 1,\ d_B = D_B/D_A,\ T = D_At/L^2,$$
$$U = Lur^2/(D_Aa^2),\ K_f = L^2k_fC_{A0}^2/D_A,$$

and

$$K_b = k_b^*L^2/C_{A0}D_A. \quad (16)$$

In the above, L is the representative length and H a constant. The maximum value of s is unity, where the value of r is infinite. With these transformations, Eq. 5 becomes

$$\frac{\partial y_A}{\partial T} = d_AH^2(1 - s^P)^{2(P+1)/P}\frac{\partial^2 y_A}{\partial s^2} + 2H(1 - s^P)^{(P+1)/P}\left\{\frac{2d_A}{x + a/L} + \frac{x(x + 2a/L)}{(x + a/L)^2}U - 2d_AH(P + 1)s^{P-1}(1 - s^P)^{1/P}\right\}\frac{\partial y_A}{\partial s} - K_fy_Ay_B^2 + K_b. \quad (17)$$

Derivation of Eq. 17 is carried out with the aid of the Crank-Nicolson's method[5] in a similar manner as the previous report. Space and time coordinates are expressed as

$$s_i = i\Delta s,\ T_j = j\Delta T,\ x_i = i\Delta s/H\{1 + (i\Delta s)^P\}^{1/P}, \quad (18)$$

and

$$y_A(s,T) = y_A(s_i, T_j) = y_{A,i,j}. \quad (19)$$

When the value of Δs is 0.01, the value of i ranges from 0, corresponding to the electrode surface, to 100, corresponding to infinite distance from the surface. The backward space difference method and the forward time difference method[2] are used in conversion of differential equations to difference equations.

In the case that $0<i<98$, the derivatives corresponding to both $\partial y_A(s,T)/\partial s$ and $\partial^2 y_A(s,T)/\partial s^2$ are expressed as

$$\left(\frac{\partial^2 y_A(s_i, T_{j+1})}{\partial s^2}\right) = \frac{1}{24(\Delta s)^2}\{(-y_{A,i+3,j+1} + 4y_{A,i+2,j+1} + 6y_{A,i+1,j+1} - 20y_{A,i,j+1} + 11y_{A,i-1,j+1}) + (-y_{A,i+3,j} + 4y_{A,i+2,j} + 6y_{A,i+1,j} - 20y_{A,i,j} + 11y_{A,i-1,j})\}, \quad (20)$$

and

$$\left(\frac{\partial y_A(s_i, T_{j+1})}{\partial s}\right) = \frac{1}{24\Delta s}\{(y_{A,i+3,j+1} - 6y_{A,i+2,j+1} + 18y_{A,i+1,j+1} - 10y_{A,i,j+1} - 3y_{A,i-1,j+1}) + (y_{A,i+3,j} - 6y_{A,i+2,j} + 18y_{A,i+1,j} - 10y_{A,i,j} - 3y_{A,i-1,j})\}, \quad (21)$$

with concentrations at the nodes $(i-1,j)$, (i,j), $(i+1,j)$, $(i+2,j)$, $(i+3,j)$, $(i-1,j+1)$, $(i,j+1)$, $(i+1,j+1)$, $(i+2,j+1)$, and $(i+3,j+1)$.

For the point that $i=98$, the outer nodes are ones with i of 99 and 100. Therefore, the backward space difference method was not applicable for conversion. The centered space difference method was used for this purpose. The derivatives are expressed as

$$\left(\frac{\partial^2 y_A(s_{98}, T_{j+1})}{\partial s^2}\right) = \frac{1}{24(\Delta s)^2}\{(-y_{A,100,j+1} + 16y_{A,99,j+1} - 30y_{A,98,j+1} + 16y_{A,97,j+1} - y_{A,96,j+1}) + (-y_{A,100,j} + 16y_{A,99,j} - 30y_{A,98,j} + 16y_{A,97,j} - y_{A,96,j})\}, \quad (22)$$

and

$$\left(\frac{\partial y_A(s_{98}, T_{j+1})}{\partial s}\right) = \frac{1}{24\Delta s}\{(-y_{A,100,j+1} + 8y_{A,99,j+1} - 8y_{A,97,j+1} + y_{A,96,j+1}) + (-y_{A,100,j} + 8y_{A,99,j} - 8y_{A,97,j} + y_{A,96,j})\}, \quad (23)$$

with concentrations at nodes $(96,j)$, $(97,j)$, $(98,j)$, $(99,j)$, $(100,j)$, $(96,j+1)$, $(97,j+1)$, $(98,j+1)$, $(99,j+1)$, and $(100,j+1)$.

For the point that $i=99$, the only outer node is a node with i of 100. Therefore, the forward space difference method was used for this purpose. The derivatives are expressed as

$$\left(\frac{\partial^2 y_A(s_{99}, T_{j+1})}{\partial s^2}\right) = \frac{1}{24(\Delta s)^2}\{(11y_{A,100,j+1} - 20y_{A,99,j+1} + 6y_{A,98,j+1} + 4y_{A,97,j+1} - y_{A,96,j+1}) + (11y_{A,100,j} - 20y_{A,99,j} + 6y_{A,98,j} + 4y_{A,97,j} - y_{A,96,j})\}, \quad (24)$$

and

$$\left(\frac{\partial y_A(s_{99}, T_{j+1})}{\partial s}\right) = \frac{1}{24\Delta s}\{(3y_{A,100,j+1} + 10y_{A,99,j+1} - 18y_{A,98,j+1} + 6y_{A,97,j+1} - y_{A,96,j+1}) + (3y_{A,100,j} + 10y_{A,99,j} - 18y_{A,98,j} + 6y_{A,97,j} - y_{A,96,j})\}. \quad (25)$$

with concentrations at the nodes $(96,j)$, $(97,j)$, $(98,j)$, $(99,j)$, $(100,j)$, $(96,j+1)$, $(97,j+1)$, $(98,j+1)$, $(99,j+1)$, and $(100,j+1)$.

By using the Crank-Nicolson method, the chemical kinetics term is reformulated as

$$K_f y_A y_b^2 = K_f(y_{A,i,j+1}y_{B,i,j+1}^2 + y_{A,i,j}y_{B,i,j}^2)/2. \quad (26)$$

Because the right-hand side of Eq. 26 contains square of $y_{B,ij+1}$, the value of y_B at the next time coordinate, it is difficult to perform numerical computation without rewriting the term in linear form with respect to $y_{B,ij+1}$. Linearization of the chemical kinetics term was treated in the previous report, where four methods were described. Larger reaction rate prevents computing by use of these methods because of truncation error. Considering large values of precipitation reaction rate constant (k_f) and dissolution rate constant (k_b) in the present system, the procedure proposed by Morihara and Cheng is applied to the present problem.[3]

By using the method of Morihara and Cheng, the chemical kinetics term is reformulated as follows:

$$K_f(y_{A,i,j+1}y_{B,i,j+1}^2 + y_{A,i,j}y_{B,i,j}^2)/2 = K_f y_{B,i,j+1}y_{B,i,j}(y_{A,i,j+1} + y_{A,i,j})/2. \quad (27)$$

When $0<i<98$, introduction of Eqs. 20, 21, and 27 to Eq. 17 gives

$$\begin{aligned}(1 &+ 20E_{A,i} + 10F_{A,i,j+1} + \Delta TK_f y_{B,i,j+1}y_{B,i,j}/2)y_{A,i,j+1} \\ &= (-E_{A,i} + F_{A,i,j+1})(y_{A,i+3,j+1} + y_{A,i+3,j}) \\ &+ (4E_{A,i} - 6F_{A,i,j+1})(y_{A,i+2,j+1} + y_{A,i+2,j}) \\ &+ (6E_{A,i} + 18F_{A,i,j+1})(y_{A,i+1,j+1} + y_{A,i+1,j}) \\ &+ (11E_{A,i} - 3F_{A,i,j+1})(y_{A,i-1,j+1} + y_{A,i-1,j}) \\ &+ (1 - 20E_{A,i} + 10F_{A,i,j+1} \\ &- \Delta TK_f y_{B,i,j+1}y_{B,i,j}/2)y_{A,i,j} + \Delta TK_b, \end{aligned} \quad (28)$$

$$E_{A,i} = \frac{\Delta T}{24\Delta s^2} d_A H^2\{1 - (s_i)^P\}^{2(P+1)/P}, \quad (29)$$

and

$$F_{A,i,j+1} = \frac{\Delta T}{12\Delta s}\left[H\{1-(s_i)^P\}^{(P+1)/P} + \frac{d_A}{x_i + a_{j+1}/L} + \frac{x_i(x_i+2a_{j+1}/L)}{2(x_i+a_{j+1}/L)^2}U_{j+1} - \frac{d_A}{2}H(P+1)\{1-(s_i)^P\}^{1/P}\right]. \quad (30)$$

When i=98, introduction of Eqs. 22, 23, and 27 to Eq. 17 gives

$$\begin{aligned}&(1 + 30E_{A,98} + \Delta TK_f y_{B,98,j+1}y_{B,98,j}/2)y_{A,98,j+1}\\ &= (-E_{A,98} - F_{A,98,j+1})(y_{A,100,j+1} + y_{A,100,j})\\ &+ (16E_{A,98} + 8F_{A,98,j+1})(y_{A,99,j+1} + y_{A,99,j})\\ &+ (16E_{A,98} - 8F_{A,98,j+1})(y_{A,97,j+1} + y_{A,97,j})\\ &+ (-E_{A,98} - 3F_{A,98,j+1})(y_{A,96,j+1} + y_{A,96,j})\\ &+ (1 - 30E_{A,98} - \Delta TK_f y_{B,i,j+1}y_{B,i,j}/2)y_{A,i,j}\\ &+ \Delta TK_b. \end{aligned} \quad (31)$$

When i=99, introduction of Eqs. 24, 25, and 27 to Eq. 17 gives

$$\begin{aligned}&(1 + 20E_{A,99} - 10F_{A,99,j+1}\\ &+ \Delta TK_f y_{B,99,j+1}y_{B,99,j}/2)y_{A,99,j+1}\\ &= (11E_{A,99} + 3F_{A,99,j+1})(y_{A,100,j+1} + y_{A,100,j})\\ &+ (6E_{A,99} - 18F_{A,99,j+1})(y_{A,98,j+1} + y_{A,98,j})\\ &+ (4E_{A,98} + 6F_{A,99,j+1})(y_{A,97,j+1} + y_{A,97,j})\\ &+ (-E_{A,99} - F_{A,99,j+1})(y_{A,96,j+1} + y_{A,96,j})\\ &+ (1 - 20E_{A,98} + 10F_{A,99,j+1}\\ &- \Delta TK_f y_{B,99,j+1}y_{B,99,j}/2)y_{A,99,j} + \Delta TK_b. \end{aligned} \quad (32)$$

The equation concerning species B is transformed as described below.

In the case that i=0, the boundary condition corresponding to $(\partial y_B/\partial s)_{r=a}$=0 is expressed as

$$\left(\frac{\partial C_B(s_0, T_{j+1})}{\partial s}\right) = \frac{1}{6(\Delta s)}(-11y_{B,0,j+1} + 18y_{B,1,j+1} - 9y_{B,2,j+1} + 2y_{B,3,j+1}) = 0, \quad (33)$$

with the concentration at nodes (0,j), (1,j), (2,j), (3,j), (0,j+1), (1,j+1), (2,j+1), and (3,j+1). The following equation is obtained from Eq. 33.

$$y_{B,0,j+1} = (18y_{B,1,j+1} - 9y_{B,2,j+1} + 2y_{B,3,j+1})/11 \quad (34)$$

In the case that i=1, the derivative corresponding to $\partial y_B/\partial s$ is expressed as

$$\begin{aligned}\left(\frac{\partial^2 y_B(s_1, T_{j+1})}{\partial s^2}\right) = \frac{1}{276(\Delta s)^2}\{&(-4y_{B,4,j+1} + 6y_{B,3,j+1}\\ &+ 159y_{B,2,j+1} - 350y_{B,1,j+1} + 189y_{B,0,j+1}\\ &+ 30(\Delta s)y'_{B,0,j+1} + (-4y_{B,4,j} + 6y_{B,3,j}\\ &+ 159y_{B,2,j} - 350y_{B,1,j} + 189y_{B,0,j}\\ &+ 30(\Delta s)y'_{B,0,j})\}, \end{aligned} \quad (35)$$

and

$$\begin{aligned}\left(\frac{\partial y_B(s_1, T_{j+1})}{\partial s}\right) = \frac{1}{444(\Delta s)}\{&(-4y_{B,4,j+1} + 9y_{B,3,j+1}\\ &+ 63y_{B,2,j+1} + 175y_{B,1,j+1} - 243y_{B,0,j+1}\\ &- 90(\Delta s)y'_{B,0,j+1}) + (-4y_{B,4,j} + 9y_{B,3,j}\\ &+ 63y_{B,2,j} + 175y_{B,1,j} - 243y_{B,0,j}\\ &- 90(\Delta s)y'_{B,0,j})\}, \end{aligned} \quad (36)$$

with the first differential term at the mercury electrode surface ($y'_{B,0,j+1}$, $y'_{B,0,j}$) and with concentrations at nodes (0,j), (1,j), (2,j), (3,j), (4,j), (0,j+1), (1,j+1), (2,j+1), (3,j+1), and (4,j+1). Here values of $y'_{B,0,j+1}$ and $y'_{B,0,j}$ are zero because the chloride ions do not receive any electrochemical change. Introduction of Eqs. 27, 35, and 36 to Eq. 6 gives

$$\begin{aligned}&\{1 + 700E_{B,1}/23 - 350F_{B,1,j+1}/37\\ &+ \Delta TK_f y_{B,1,j}(y_{A,1,j+1} + y_{A,1,j})/2\}y_{B,1,j+1}\\ &= (-8E_{B,1}/23 - 8F_{B,1,j+1}/37)(y_{B,4,j+1} + y_{B,4,j})\\ &+ (12E_{B,1}/23 + 18F_{B,1,j+1}/37)(y_{B,3,j+1} + y_{B,3,j})\\ &+ (318E_{B,1}/23 + 126F_{B,1,j+1}/37)(y_{B,2,j+1} + y_{B,2,j})\\ &+ (378E_{B,1}/23 - 486F_{B,1,j+1}/37)(y_{B,0,j+1} + y_{B,0,j})\\ &+ (1 - 700E_{B,1}/23 + 350F_{B,1,j+1})y_{B,1,j} + 2\Delta TK_b. \end{aligned} \quad (37)$$

When 1<i, the equations concerning with species B are transformed in much the same way as species A. Equations correspoding to Eqs. 28, 31, and 32 are given as follows:

1<i<98,

$$\begin{aligned}&\{1 + 20E_{B,i} + 10F_{B,i,j+1}\\ &+ \Delta TK_f y_{B,i,j}(y_{A,i,j+1} + y_{A,i,j})/2\}y_{B,i,j+1}\\ &= (-E_{B,i} + F_{B,i,j+1})(y_{B,i+3,j+1} + y_{B,i+3,j})\\ &+ (4E_{B,i} - 6F_{B,i,j+1})(y_{B,i+2,j+1} + y_{B,i+2,j})\\ &+ (6E_{B,i} + 18F_{B,i,j+1})(y_{B,i+1,j+1} + y_{B,i+1,j})\\ &+ (11E_{B,i} - 3F_{B,i,j+1})(y_{B,i-1,j+1} + y_{B,i-1,j})\\ &+ (1 - 20E_{B,i} - 10F_{B,i,j+1})y_{B,i,j} + 2\Delta TK_b. \end{aligned} \quad (38)$$

i=98,

$$\begin{aligned}&\{1 + 30E_{B,98} + \Delta TK_f y_{B,98,j}(y_{A,98,j+1}\\ &+ y_{A,98,j})/2\}y_{B,98,j+1}\\ &= (-E_{B,98} - F_{B,98,j+1})(y_{B,100,j+1} + y_{B,100,j})\\ &+ (16E_{B,98} + 8F_{B,98,j+1})(y_{B,99,j+1} + y_{B,99,j})\\ &+ (16E_{B,98} - 8F_{B,98,j+1})(y_{B,97,j+1} + y_{B,97,j})\\ &+ (-E_{B,98} - 3F_{B,98,j+1})(y_{B,96,j+1} + y_{B,96,j})\\ &+ (1 - 30E_{B,98})y_{B,i,j} + 2\Delta TK_b. \end{aligned} \quad (39)$$

i=99,

$$\begin{aligned}&\{1 + 20E_{B,99} - 10F_{B,99,j+1} + \Delta TK_f y_{B,99,j}(y_{A,99,j+1}\\ &+ y_{A,99,j})/2\}y_{B,99,j+1}\\ &= (11E_{B,99} + 3F_{B,99,j+1})(y_{A,100,j+1} + y_{B,100,j})\\ &+ (6E_{B,99} - 18F_{B,99,j+1})(y_{B,98,j+1} + y_{B,98,j})\\ &+ (4E_{B,99} + 6F_{B,99,j+1})(y_{B,97,j+1} + y_{B,97,j})\\ &+ (-E_{B,99} - F_{B,99,j+1})(y_{B,96,j+1} + y_{B,96,j})\\ &+ (1 - 20E_{B,98} + 10F_{B,99,j+1})y_{A,i,j} + \Delta TK_b. \end{aligned} \quad (40)$$

In the volume element, where $C_A C_B^2 < K_{sp}$ is hold, Eqs. 5 and 6 are replaced by Eqs. 9 and 10, respectively. By neglecting chemical kinetics terms in Eqs. 28, 31, 32, 37, 38, 39, and 40, the finite difference equations are given as follows:

$0<i<98$,

$$\begin{aligned}(1 &+ 20E_{A,i} + 10F_{A,i,j+1})y_{A,i,j+1}\\ &= (-E_{A,i} + F_{A,i,j+1})(y_{A,i+3,j+1} + y_{A,i+3,j})\\ &+ (4E_{A,i} - 6F_{A,i,j+1})(y_{A,i+2,j+1} + y_{A,i+2,j})\\ &+ (6E_{A,i} + 18F_{A,i,j+1})(y_{A,i+1,j+1} + y_{A,i+1,j})\\ &+ (11E_{A,i} - 3F_{A,i,j+1})(y_{A,i-1,j+1} + y_{A,i-1,j})\\ &+ (1 + 20E_{A,i} + 19F_{A,i,j+1})y_{A,i,j}. \end{aligned} \quad (41)$$

$i=98$,

$$\begin{aligned}(1 &+ 30E_{A,98})y_{A,98,j+1}\\ &= (-E_{A,98} - F_{A,98,j+1})(y_{A,100,j+1} + y_{A,100,j})\\ &+ (16E_{A,98} + 8F_{A,98,j+1})(y_{A,99,j+1} + y_{A,99,j})\\ &+ (16E_{A,98} - 8F_{A,98,j+1})(y_{A,97,j+1} + y_{A,97,j})\\ &+ (-E_{A,98} - 3F_{A,98,j+1})(y_{A,96,j+1} + y_{A,96,j})\\ &+ (1 - 30E_{A,98})y_{A,98,j}. \end{aligned} \quad (42)$$

$i=99$,

$$\begin{aligned}(1 &+ 20E_{A,99} - 10F_{A,99,j+1})y_{A,99,j+1}\\ &= (11E_{A,99} + 3F_{A,99,j+1})(y_{A,100,j+1} + y_{A,100,j})\\ &+ (6E_{A,99} - 18F_{A,99,j+1})(y_{A,98,j+1} + y_{A,98,j})\\ &+ (4E_{A,99} + 6F_{A,99,j+1})(y_{A,97,j+1} + y_{A,97,j})\\ &+ (-E_{A,99} - F_{A,99,j+1})(y_{A,96,j+1} + y_{A,96,j})\\ &+ (1 - 20E_{A,98} + 10F_{A,99,j+1})y_{A,99,j}. \end{aligned} \quad (43)$$

$i=0$,

$$y_{B,0,j+1} = (18y_{B,1,j+1} - 9y_{B,2,j+1} + 2y_{B,3,j+1})/11. \quad (44)$$

$i=1$,

$$\begin{aligned}(1 &+ 700E_{B,1}/23 - 350F_{B,1,j+1}/37)y_{B,1,j}\\ &= (-8E_{B,1}/23 - 8F_{B,1,j+1}/37)(y_{B,4,j+1} + y_{B,4,j})\\ &+ (12E_{B,1}/23 + 18F_{B,1,j+1}/37)(y_{B,3,j+1} + y_{B,3,j})\\ &+ (318E_{B,1}/23 + 126F_{B,1,j+1}/37)(y_{B,2,j+1} + y_{B,2,j})\\ &+ (378E_{B,1}/23 - 486F_{B,1,j+1}/37)(y_{B,0,j+1} + y_{B,0,j})\\ &+ (1 - 700E_{B,1}/23 + 350F_{B,1,j+1})y_{B,1,j}. \end{aligned} \quad (45)$$

$1<i<98$,

$$\begin{aligned}(1 &+ 20E_{B,i} + 10F_{B,i,j+1})y_{B,i,j+1}\\ &= (-E_{B,i} + F_{B,i,j+1})(y_{B,i+3,j+1} + y_{B,i+3,j})\\ &+ (4E_{B,i} - 6F_{B,i,j+1})(y_{B,i+2,j+1} + y_{B,i+2,j})\\ &+ (6E_{B,i} + 18F_{B,i,j+1})(y_{B,i+1,j+1} + y_{B,i+1,j})\\ &+ (11E_{B,i} - 3F_{B,i,j+1})(y_{B,i-1,j+1} + y_{B,i-1,j})\\ &+ (1 - 20E_{B,i} - 10F_{B,i,j+1})y_{B,i,j}. \end{aligned} \quad (46)$$

$i=98$,

$$\begin{aligned}(1 &+ 30E_{B,98})y_{B,98,j+1}\\ &= (-E_{B,98} - F_{B,98,j+1})(y_{B,100,j+1} + y_{B,100,j})\\ &+ (16E_{B,98} + 8F_{B,98,j+1})(y_{B,99,j+1} + y_{B,99,j})\\ &+ (16E_{B,98} - 8F_{B,98,j+1})(y_{B,97,j+1} + y_{B,97,j})\\ &+ (-E_{B,98} - 3F_{B,98,j+1})(y_{B,96,j+1} + y_{B,96,j})\\ &+ (1 - 30E_{B,98})y_{B,98,j}. \end{aligned} \quad (47)$$

$i=99$,

$$\begin{aligned}(1 &+ 20E_{B,99} - 10F_{B,99,j+1})y_{B,99,j+1}\\ &= (11E_{B,99} + 3F_{B,99,j+1})(y_{B,100,j+1} + y_{B,100,j})\\ &+ (6E_{B,99} - 18F_{B,99,j+1})(y_{B,98,j+1} + y_{B,98,j})\\ &+ (4E_{B,99} + 6F_{B,99,j+1})(y_{B,97,j+1} + y_{B,97,j})\\ &+ (-E_{B,99} - F_{B,99,j+1})(y_{B,96,j+1} + y_{B,96,j})\\ &+ (1 - 20E_{B,98} + 10F_{B,99,j+1})y_{A,99,j}. \end{aligned} \quad (48)$$

In the above, the value of $y_{A,i,j+1}$ is calculated by Eqs. 28, 31, 32, and 41—43, and the value of $y_{B,i,j+1}$ by Eqs. 34, 37—40, and 45—48.

Equation 7 concerning species C contains a fluid flow term resulted from the growth of the mercury drop, but no diffusion term. The surface of electrode drop moves outward with time, and the solution around the drop flows from the outer regions to the surface of electrode. Hence concentrations at outer nodes control future concentrations at inner nodes. By this reason it is vital to use the backward space difference method for reformulation of the equation. This is contrary to other equations which contain diffusion terms. In diffusion, concentrations of both the inner and outer nodes are important factors determining their future concentrations. Hence, all the forward, centered, and backward space difference methods can be used for reformulation of an equation containing both the fluid flow and diffusion terms. In this paper, backward space difference method is used as shown in reformulation of Eqs. 5 and 6.

For transformation of Eq. 7 to difference equation, the derivatives are rewritten as shown below.

In the case that $i=1$, the derivative corresponding to $\partial C_C/\partial r$ is expressed as

$$\begin{aligned}\left(\frac{\partial y_C(s_1, T_{j+1})}{\partial s}\right) &= \frac{1}{24\Delta s}\{(-3y_{C,5,j+1} + 16y_{C,4,j+1}\\ &- 36y_{C,3,j+1} + 48y_{C,2,j+1} - 25y_{C,1,j+1}) + (-3y_{C,5,j+1}\\ &+ 16y_{C,4,j+1} - 36y_{C,3,j+1} + 48y_{C,2,j+1} - 25y_{C,1,j+1})\}, \end{aligned} \quad (49)$$

with the concentrations at the nodes $(1,j)$, $(2,j)$, $(3,j)$, $(4,j)$, $(5,j)$, $(1,j+1)$, $(2,j+1)$, $(3,j+1)$, $(4,j+1)$, and $(5,j+1)$.

When $1<i<98$, the derivative is expressed as

$$\begin{aligned}\left(\frac{\partial y_C(s_i, T_{j+1})}{\partial s}\right) &= \frac{1}{24\Delta s}\{(y_{C,i+3,j+1} - 6y_{C,i+2,j+1}\\ &+ 18y_{C,i+1,j+1} - 10y_{C,i,j+1} - 3y_{C,i-1,j+1})\\ &+ (-y_{C,i+3,j} - 6y_{C,i+2,j} + 18y_{C,i+1,j} - 10y_{C,i,j}\\ &- 3y_{C,i-1j})\}, \end{aligned} \quad (50)$$

with the concentrations at the nodes $(i-1,j)$, (i,j), $(i+1,j)$, $(i+2,j)$, $(i+3,j)$, $(i-1,j+1)$, $(i,j+1)$, $(i+1,j+1)$,

$(i+2,j+1)$, and $(i+3,j+1)$.

When a point has i of 98, the outer nodes are those with i of 99 and 100. Therefore, application of the backward space difference method is impossible. The point is well distant from the electrode surface and the moment of the surface does not cause any significant effect. By this reason, the centered space difference method was used for transformation. The derivative is expressed with the concentrations at the nodes $(96,j)$, $(97,j)$, $(98,j)$, $(99,j)$, $(100,j)$, $(96,j+1)$, $(97,j+1)$, $(98,j+1)$, $(99,j+1)$, and $(100,j+1)$.

$$\left(\frac{\partial y_{C}(s_{98}, T_{j+1})}{\partial s}\right) = \frac{1}{24\Delta s}\{(-y_{C,100,j+1} + 8y_{C,99,j+1} - 8y_{C,97,j+1} + y_{C,96,j+1}) + (-y_{C,100,j} + 8y_{C,99,j} - 8y_{C,97,j} + y_{C,96,j})\}. \quad (51)$$

For the point that $i=99$, the only outer node is one with i of 100. Therefore, application of both the centered and backward space difference methods are impossible. The forward space difference method was used for this purpose. The derivative is expressed with the concentrations at the nodes $(96,j)$, $(97,j)$, $(98,j)$, $(99,j)$, $(100,j)$, $(96,j+1)$, $(97,j+1)$, $(98,j+1)$, $(99,j+1)$, and $(100,j+1)$.

$$\left(\frac{\partial y_{C}(s_{99}, T_{j+1})}{\partial s}\right) = \frac{1}{24\Delta s}\{(3y_{C,100,j+1} + 10y_{C,99,j+1} - 18y_{C,98,j+1} + 6y_{C,97,j+1} - y_{C,96,j}) + (3y_{C,100,j} + 10y_{C,99,j} - 18y_{C,98,j} + 6y_{C,97,j} - y_{C,96,j})\}. \quad (52)$$

Introducing Eqs. 49—52 into Eq. 7, we have the following equations:

$i=1$,

$$(1 + 25P_{C,1,j+1})y_{C,1,j+1} = P_{C,1,j+1}\{(-3y_{C,5,j+1} + 16y_{C,4,j+1} - 36y_{C,3,j+1} + 48y_{C,2,j+1}) + (-3y_{C,5,j} + 16y_{C,4,j} - 36y_{C,3,j} + 48y_{C,2,j} - 25y_{C,1,j})\} + y_{C,1,j} + \Delta TK_{f}y_{B,1,j+1}y_{B,1,j}(y_{A,1,j+1} + y_{A,1,j})/2 - \Delta TK_{b}. \quad (53)$$

$1<i<98$,

$$(1 + 10P_{C,i,j+1})y_{C,i,j+1} = P_{C,i,j+1}\{(y_{C,i+3,j+1} - 6y_{C,i+2,j+1} + 18y_{C,i+1,j+1} - 3y_{C,i-1,j+1}) + (y_{C,i+3j} - 6y_{C,i+2,j} + 18y_{C,i+1,j} - 10y_{C,i,j} - 3y_{C,i-1,j})\} + y_{C,i,j} + \Delta TK_{f}y_{B,i,j+1}y_{B,i,j}(y_{A,i,j+1} + y_{A,i,j})/2 - \Delta TK_{b}. \quad (54)$$

$i=98$,

$$y_{C,98,j+1} = P_{C,98,j+1}\{(-y_{C,100,j+1} + 8y_{C,99,j+1} - 8y_{C,97,j+1} + y_{C,96,j+1}) + (-y_{C,100,j} + 8y_{C,99,j} - 8y_{C,97,j} + y_{C,96,j})\} + y_{C,98,j} + \Delta TK_{f}y_{B,98,j+1}y_{B,98,j}(y_{A,98,j+1} + y_{A,98,j})/2 - \Delta TK_{b}. \quad (55)$$

$i=99$,

$$(1 - 10P_{C,99,j+1})y_{C,99,j+1} = P_{C,99,j+1}\{(3y_{C,100,j+1} - 18y_{C,98,j+1} + 6y_{C,97,j+1} - y_{C,96,j+1}) + (3y_{C,100,j} + 10y_{C,99,j} - 18y_{C,98,j} + 6y_{C,97,j} - y_{C,96,j})\} + y_{C,99,j} + \Delta TK_{f}y_{B,99,j+1}y_{B,99,j}(y_{A,99,j+1} + y_{A,99,j})/2 - \Delta TK_{b}. \quad (56)$$

$$P_{C,i,j+1} = \frac{\Delta TH(1 - s_i)^2U_{j+1}x_i(x_i + 2a_{j+1}/L)}{24\Delta s(x_i + a_{j+1}/L)^2}. \quad (57)$$

The value of $y_{C,i,j+1}$ is calculated with the aid of Eqs. 53—56.

The numerical computation described in the present method was programmed with the Gauss-Seidel method and the successive over relaxation method by using FORTRAN.

Converged values at $j\Delta T$ are usually used as initial values for computation of values at $(j+1)\Delta T$. This practice was successful when the concentration of chloride ions was lower than 1×10^{-4} mol dm^{-3}, where the difference between concentrations of mercury(I) and chloride ions was moderate. It produced, however, tremendous increase in the number of repetitions when the difference between concentrations of mercury(I) and chloride ions became large. It was nearly prohibitive. Therefore a new procedure was used instead of the practice described above. It was by use of estimated values at $(j+1)\Delta T$ as initial values for computation. The values at $(j+1)\Delta T$ are estimated roughly with the assumption that the converged values at $(j+1)\Delta T$ are situated on the extension of the line connecting two points, $y_{A,i,j-1}$ and $y_{A,i,j}$ The initial values at $(j+1)\Delta T$ are estimated with the following equations:

$$y_{A,i,j+1} = R(y_{A,i,j} - y_{A,i,j-1}) + y_{A,i,j}, \quad (58)$$

where R is a constant ranging from 0.1 to 1.01.

Up to this point, consideration is confined solely to the current corresponding to the observed current. The residual current should be considered next. Because the residual current is the current in the absence of the chloride ion, the differential equation to be used for calculation of the residue current is Eq. 9, of which difference equation forms are Eqs. 41—43. Initial condition is

$$C_{A} = 0 (t = 0, \quad r > a). \quad (59)$$

Boundary conditions are

$$C_{A} = C_{A0} (t > 0, \quad r = a), \quad (60)$$

$$C_{A} = 0 (t > 0, \quad r = \infty). \quad (61)$$

The instantaneous anodic current in the absence of chloride ions, i_r, is given by

$$i_r = 2FD_{A}S(\partial C_{A}/\partial r)_{r=a}. \quad (62)$$

Kolthoff and Miller corrected the observed current for residual current by

$$i_c = i - i_r. \quad (63)$$

The corrected current, i_c is the current mainly caused by precipitation reaction.

Results and Discussion

Any numerical method should be established by comparison of calculated results with observed data. The validity of the present method was examined under various experimental conditions. The anodic wave of mercury was measured in the presence of chloride ions of various concentrations.

The value of diffusion coefficient of mercury(I) ions for numerical computations was chosen so as to minimize difference between calculated and observed current.[2] This procedure produces a value of 0.847×10^{-5} cm^2 s^{-1}. The value of diffusion coefficient of chloride ions used is 2.03×10^{-5} cm^2 s^{-1}.[6]

Figure 2 shows the plots of $\log(i_d-i_c)$ vs. E constructed with observed data, where currents were measured at the end of life of mercury drop. The plots give straight lines. The slope of these lines ranges from −45 to −52 mV/unit. Experimental values of the reciprocal slope do not agree with Eq. 1. The half-wave potential shifts to anodic direction with increase of ionic strength. This shift is explained as follows: The concentration constant of the solubility product increases with ionic strength, because activity coefficients of ions decrease with ionic strength within the limit of the experimental conditions. The shift of half-wave potential is anodic direction as shown in Eq. 1. The value of anodic current corrected for residual current was proportional to the concentration of chloride ions.

Figure 3 shows the effect of concentration of ethanol added to the electrolyte. The concentration of ethanol does not influence on the value of reciprocal slope. However, the half-wave potential of anodic wave shifts to more negative by 52 mV with increase in the concentration of ethanol from 0 to 40 vol%, because the solubility product of mercury(I) chloride decrease with increase of ethanol concentration. The plots of $\log(i_d-i_c)$ vs. E produce straight lines with slopes ranging from −45 to −52 mV/unit.

Computation of the anodic current by the method described in Theory was successful when the concentration of chloride ions was within the range of 10^{-5} to 3×10^{-4} mol dm^{-3}. Values of parameters used are as follows: The value of L ranges from 10^{-5} to 10^{-2} cm and ΔT from 4.27×10^{-7} to 2.18×10^{-4} s. The rate constant of precipitate particle formation was chosen as the value of $C_AC_B^2$ in each volume element does not exceed the solubility product by as much as 10%. The computation failed, however, when the concentration of chloride ions was over 3×10^{-4} mol dm^{-3}. The reason of failure is as follows: The anodic wave caused by precipitation appears at the electrode potential ranging from 0.25 to 0.30 V vs. SCE. The concentration of mercury(I) ions in contact with mercury electrode at 0.30 V vs. SCE is 2.1×10^{-9} mol dm^{-3}, which is far lower than that of chloride ions. Remarkable imbalance between concentrations of mercury(I) and chloride ions prevents successful computation, even if it is performed with double precision.

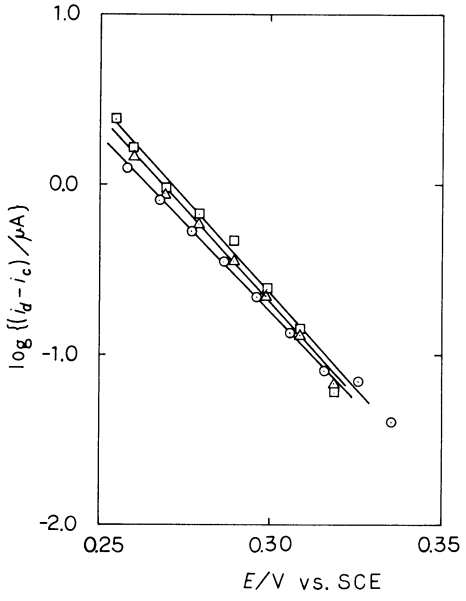

Fig. 2. Effect of ionic strength on the anodic wave in the solution of 0.5×10^{-3} mol dm^{-3} KCl and 0.005% gelatin. Value of ionic strength: ○, 0.05 M; △, 0.1 M; □, 0.2 M. The ionic strength is adjusted with potassium nitrate.

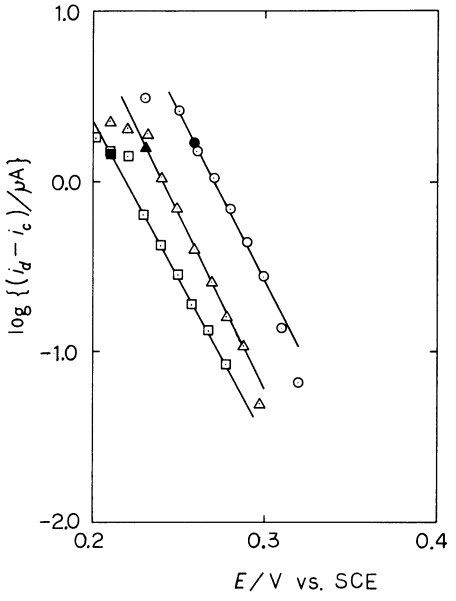

Fig. 3. Effect of the concentration of ethyl alcohol on the anodic wave in the solution containing 0.5×10^{-3} mol dm^{-3} KCl, 0.05 mol dm^{-3} KNO_3, and 0.005% gelatin. Concentration of ethyl alcohol: ○, 0 vol%; △, 20 vol%; □, 40 vol%. Filled symbols indicate the half-wave potentials.

Figure 4 shows the plots of $\log(i_d-i_c)$ vs. E constructed with calculated and observed data. The calculated data are consistent with the observed ones in the case that the concentration of chloride ions is 1×10^{-4} and 3×10^{-4} mol dm^{-3}.

Figure 5 shows the plot of the corrected limiting currents, i_l, vs. concentration of chloride ions. The current is proportional to the concentration. The points corresponding to calculated and observed limiting currents are on a straight line. The plot of observed half-wave potential against the logarithm of concentration of chloride ions produces another straight line. The value of slope of the straight line is -59 mV/unit, and this value agrees with the theoretical value given by Eq. 1. The calculated half-wave potential values are on this line. It indicates that the present method of the calculation reflects the phenomena going on in the vicinity of dropping mercury electrode. The value of the solubility product was chosen for the computed points to be on straight lines. A chosen value of solubility product of mercury(I) chloride is 2.0×10^{-17} mol^3 dm^{-9}. After making activity correction, the value of the activity product is given as 4.04×10^{-18} mol^3 dm^{-9}. This value is about three times as large as ones given in a standard literature.[4] It shows that the solubility of fresh precipitate, whose age is within the life of

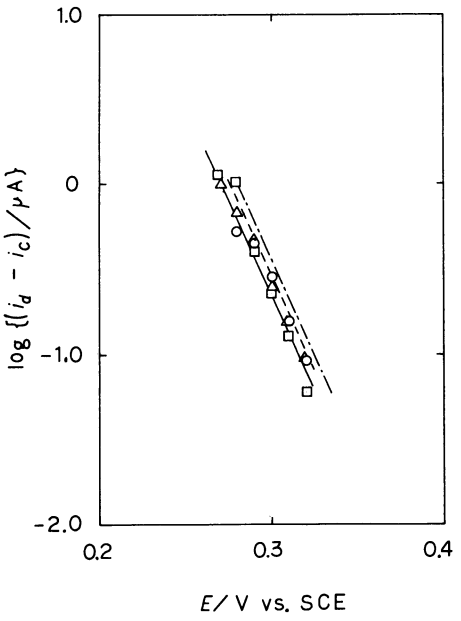

Fig. 4. Plots of E against log (i_d-i) in the solution of pH 1.93 containing 0.005% gelatin. Concentration of chloride ($\times10^{-3}$ mol dm^{-3}): (observed) O, 0.1; △, 0.2; □, 0.3; (computed), —·—, 0.1; ——, 0.2; ——, 0.3.

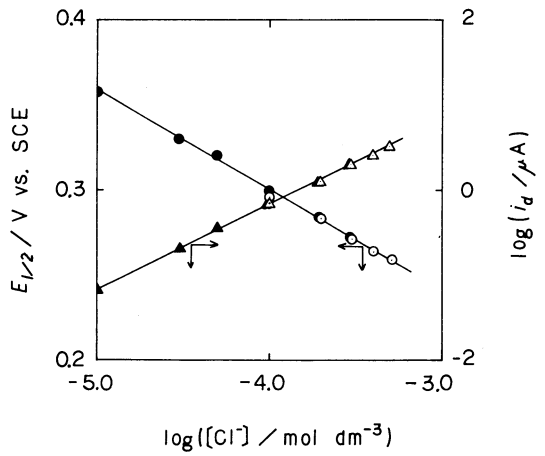

Fig. 5. Effect of chloride ions on the half-wave potential and the limiting current in the solution of pH 1.93 containing 0.01% gelatin. ●, half-wave potential computed; O, half-wave potential observed; ▲, limiting current computed; △, limiting current observed.

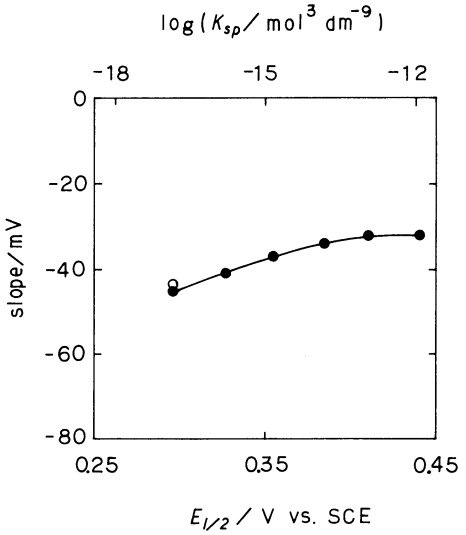

Fig. 6. Relation between the half-wave potential and the slope of logarithmic plot by the numerical method. pH 1.93 and 10^{-4} mol dm^{-3} sodium chloride. O, observed; ●, computed.

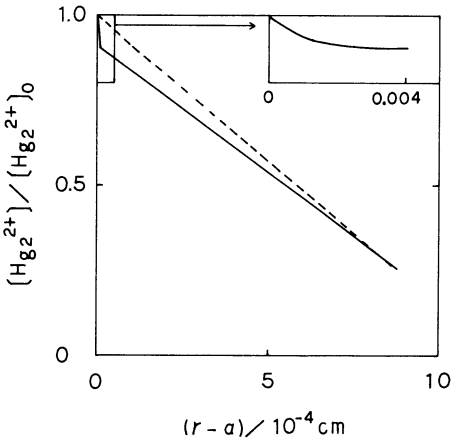

Fig. 7. Computed distance-concentration curves of mercury(I) ions at about the half-wave potential in the solution of 10^{-4} mol dm^{-3} chloride ions. The value of log (K_{sp}): a solid line, -16.7; a dotted line, -11.7. The inset shows a graph with an enlarged abscissa.

electrode mercury drop, is larger than that of more aged precipitate.

Figure 6 shows the relation among the value of solubility product, the slope of logarithmic plot, and the half-wave potential of numerically-constructed polarograms. The concentration of chloride ions was kept at 10^{-4} mol dm^{-3}. The value of slope is almost constant when the half-wave potential is more positive than 0.40 V, whereas the slope decreases to approach to -59 mV/unit when the half-wave potential becomes more negative than 0.40 V vs. SCE.

Figure 7 shows numerically constructed concentration-distance curves of mercury(I) ions at about the half-wave potential. The concentration of mercury(I) ions at the surface of electrode is 5×10^{-4} mol dm^{-3} when a value of 2×10^{-12} mol^3 dm^{-9} is used for K_{sp}, and is 5×10^{-9} mol dm^{-3} when a value of 2×10^{-17} mol^3 dm^{-9} is used. The concentration of chloride ions is identical in the above two cases. It is found that the concentration-distance curve is divided into two parts. The interior and exterior curves correspond to the regions with and without mercury(I) chloride precipitate particles, respectively. The precipitation reaction proceeds in the interior region, but does not in the exterior one. It is found that the position of boundary between two regions approaches to the surface of electrode with decrease of K_{sp}. It indicates that the thickness of layer, in which the precipitation reaction proceeds, becomes small with decrease of K_{sp}. At the limit, it produces the concentration-distance curve of chloride ions by Kolthoff and Miller, who assumed that the precipitation reaction proceeds only at the surface of electrode. Therefore the value of slope becomes -59 mV/unit with the decrease of K_{sp} shown in Fig. 6.

Experimental

The chemicals used were of reagent grade. The concentration of chloride ion in stock solutions was calculated from amounts of sodium chloride or potassium chloride dissolved. The salts were dried at 110—120 °C for 2 h. Oxygen in test solutions were expelled by bubbling pure nitrogen for 50 min. The current of the anodic wave was measured just before the detachment of mercury drop. Measurements were carried out using a Hokuto Denko Model HA 104 Potentio-Galvanostat with three electrodes arrangement at 25 °C.

The dropping mercury electrode had the following characteristics (in 0.1 mol dm^{-3} sodium perchlorate at zero applied potential vs. SCE and at a mercury head of 80.0 cm): The flow rate of mercury (m), 2.08 mg s^{-1}; the drop time (t), 3.20 s; the capillary constant ($m^{2/3}t^{1/6}$), 1.978 mg$^{2/3}$ s$^{-1/2}$.

The numerical method described in the present paper was performed by an IBM 4361-L03 computer in Shiga Prefectural Junior College.

Conclusion

The anodic wave of mercury in the presence of chloride ions was studied by a new numerical method. The boundary condition, $(\partial C_B/\partial r)_{r=a}=0$, was used for computation, because chloride ions do not participate in the charge transfer at the electrode. The differential equation for precipitate particles was transformed to the difference equation with the backward space difference method which was chosen to reflect the relative motion of the solution around the electrode mercury drop. It was found that the transformation with the backward space difference method was vital for successful computation.

The results of numerical method indicate that the relations between the concentration of chloride ions and the half-wave potential, and those between the concentration of chloride ions and the limiting current corrected for residual current are in fair agreement with an equation derived by Kolthoff and Miller. However, the computed value of reciprocal slope of straight lines obtained by plotting $\log(i_d-i_c)$ against E does not agree with their theory but fairly agrees with observed data. Reason of this seems that the rate of production of mercury(I) ions is controlled both by the diffusion of chloride ions and by the potential of mercury electrode.

References

1) I. M. Kolthoff and C. S. Miller, *J. Am. Chem. Soc.*, **63**, 1405, (1941). Equation 1 corresponds to Eq. 16 in the original paper. The former differs from the latter in respect of inclusion of the activity coefficient and change of symbols.

2) K. Kikuchi, *Bull. Chem. Soc. Jpn.*, **60**, 903 (1987).

3) H. Morihara and R. T. Cheng, *J. Compu. Phys.*, **11**, 550 (1973).

4) "Stability Constant of Metal Complexes," ed by L. G. Sillén and A. E. Martell, Chemical Society (1964), p. 292.

5) G. D. Smith, "Numerical Solution of Partial Differential Equations," Oxford University Press (1965).

6) I. M. Kolthoff and J. J. Lingane, "Polarography," Interscience Publishers (1952), Vol. 1, p. 52.